4 Exploring Change of River Morphology and Water Quality in the Stone Mine Areas of Dwarka River Basin, Eastern India

Indrajit Mandal and Swades Pal

Abstract

In developing countries, growing construction works encourage stone quarry and crushing activities. The middle catchment of east India's Dwarka River basin has a total of 239 quarrying and 982 crushing units, which produces huge stone dust affecting not only air but also river morphology and water quality. The present study aims to ascertain the impact of stone dust on river morphology change and water quality. The study identified growing channel bed aggradations (average: 0.02–0.52 m) due to stone dust. A multi-parametric approach based on machine learning methods like Fuzzy Inference System and Random Forest Algorithm incorporating eleven relevant parameters identified river bed accretion susceptibility due to stone dust. In all the cases 6–17% area is identified as highly susceptible zones. Sediment load is abnormally enhanced exceeding the carrying capacity of the river. River bed mining is identified as the major reason behind the loitering of the thalweg axis of the rivers. Degradation of water quality due to admixing of stone dust is as high as beyond drinkability and irrigability.

Keywords

Stone crushing · Stone dust · River bed accretion · Accretion susceptibility · River bed mining · Thalweg shifting · Water quality

4.1 Introduction

Mining operations consistently lead the developmental process (Xiang et al. 2018; Pal and Mandal 2021). In the twenty-first century, rapid urbanization, industrialization, and many developmental processes are sweeping a high-rise demand for construction materials (Minnullina and Vasiliev 2018). So, control of open-pit mining activity is a greater challenge for good sustainability of the environment (Chen et al. 2015; Lei et al. 2016; Esposito et al. 2017; Xiang et al. 2018). The assessment of the impacts of open-pit mining using geomorphologic knowledge can boost the reasons responsible for the qualitative degradations of our environment and we construct the necessary strategies for the betterment of the future generation (Toy and Hadley 1987; Wilkinson and McElroy 2007; Xu et al. 2019). Rivers are a vital aspect of an open natural system of the earth and it is constantly subject to change and transformation triggered by both natural as well as manmade agents (Nayyeri and Zandi 2018). Mining activity is such a type of

I. Mandal · S. Pal (✉)
Department of Geography, University of Gour Banga, Malda, West Bengal, India
e-mail: swadespal2017@gmail.com

I. Mandal
e-mail: indrajitgeofarakka@gmail.com

S. Mandal et al. (eds.), *Applied Geomorphology and Contemporary Issues*, Geography of the Physical Environment, https://doi.org/10.1007/978-3-031-04532-5_4

activity that changes the natural component like rivers (Festin et al. 2019; Milczarek 2019). On a global scale, river systems have been modified due to increasing sediment and nutrient loads (Xiang et al. 2018). Fluxes of stone dust, fly ash, eroded soil, and fertilizer residues also play a vital role in changing the biogeochemical characters (Holmes et al. 2012; Peña-Ortega et al. 2019) of a river. Change of habitat quality of a river due to changes in channel morphological characters like the roughness of river bed, depth of water, the slope of the bank, sediment load, etc. is also vital concerning the influx of stone dust (Hauer et al. 2013; Costea 2018; Hohensinner et al. 2018). Moreover, direct mining of stone from river beds also causes channel bed modification and changes in flow characters and biological habitat characters of the species living there over (Singh et al. 2016; Wiejaczka et al. 2018).

River water quality modification due to stone quarrying and crushing is one of the important issues in this connection (Nayyeri and Zandi 2018). A huge influx of stone dust can alter the physicochemical composition of the water (Fu et al. 2014, 2016; Qi et al. 2018; Quinn et al. 2018). So the influx of dust in a river or pond water can change physicochemical properties like turbidity, PH level, DO, COD, BOD, etc. (Calle et al. 2017; Barman et al. 2018; Affandi and Ishak 2019). Change of water quality beyond optimum level can change the habitability of species in a river and irrigability in its surrounding agricultural field (Mandal and Pal 2020). The high concentration of total dissolved solids (TDS) above 2250 ppt can make the water non-irrigable as per the Bureau of Indian Standards (BIS 1991). Irrigation with such water can change the soil composition of the agricultural land too (Trujillo-González et al. 2017; Khalid et al. 2018; Pal and Mandal 2019a) which may affect the productivity of the soil. Change in water quality directly affects the livelihood of the fishermen (Samah et al. 2019). Qualitative deterioration of water provides hardship to fish communities which are the mainstay of fishermen's economy (Lyons et al. 2016; Dembowska et al. 2018; Massi et al. 2019; Mariya et al. 2019). Pal et al. (2016) explored that due to qualitative change of water, availability of fish is diminished in Bakreshwar river of India and it also causes shifting of livelihood of the fishermen to other occupations like daily wage laborer, a rickshaw puller etc.

4.2 Study Area

The middle catchment of the Dwarka River basin (3882.71 km^2), a sub-basin of the Mayurakshi River basin, is characterized by Dharwanian sedimentary rocks (Hercynian orogeny, 360–300 million years ago) (Jha and Kapat 2009). The area is therefore extremely rich in stone and related crushing. Bedrock rivers have the potential for direct stone harvesting from the river bed. Almost 239 stone quarrying and 982 crushing centers and so many river bed mining (river bed cutting) centers there, as per the tally of 2018 and these are mostly located in the middle catchment (Pal and Mandal 2017, 2019a, b, 2020) (Fig. 4.1). These are generating a huge volume of stone dust and these are discharging into rivers. River bed stone quarrying (river bed cutting) is also going on at different sites of the rivers. All these can change the hydrological and geo-morphological characteristics of the river and other surface water bodies. In this sense, the present work aims to investigate the impacts of stone quarrying, crushing, and river bed mining on river morphology and also the water quality of the Dwarka river basin of Eastern India.

4.3 Materials and Methods

4.3.1 Methods for the Volume of Stone Dust Estimation on the River Bed

To measure the concentration of stone dust in all six tributaries, eight sites for each tributary have been selected to measure the depth of dust deposition. Direct field digging is done for

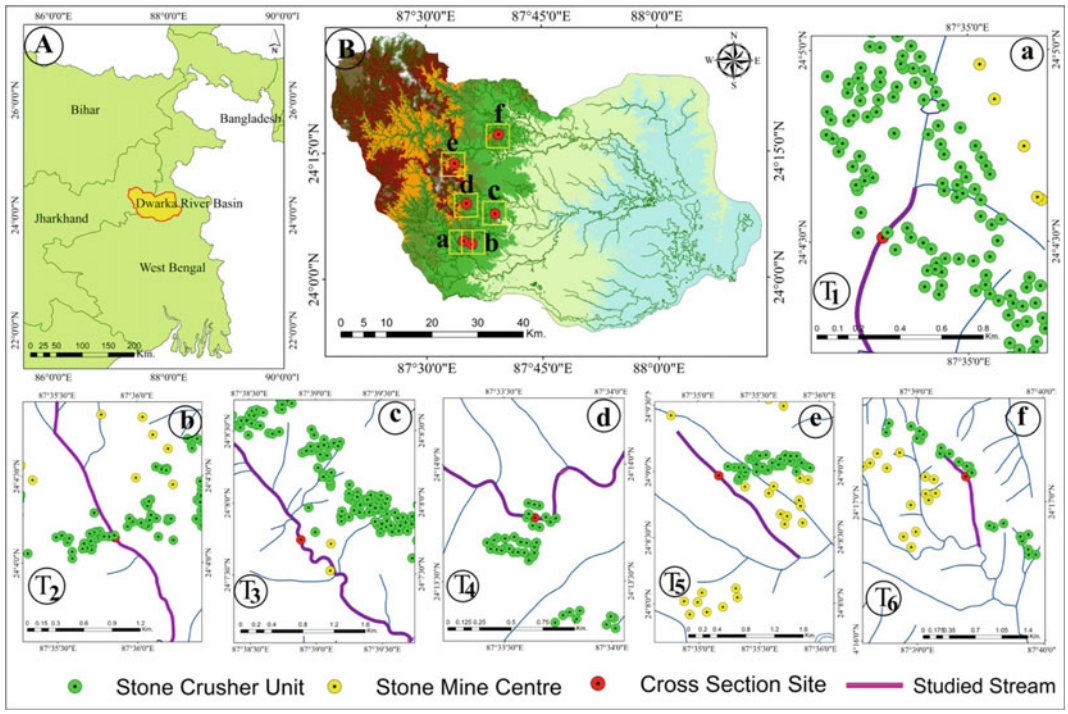

Fig. 4.1 Study area: **A** Basin extension within Jharkhand and West Bengal, **B** showing the field study site within the basin, **a**–**f** selected tributaries for the study, and cross-section site (T_1 represents tributary 1 and vice versa)

measuring the depth. The average dust depth of all sites is then multiplied by the area of the river for obtaining the total volume of dust deposition in a river.

4.3.2 Methods for Assessing Impacts on Channel Morphology

Cross-sections across the present bed level of some selected six tributary sites used a dumpy level to demonstrate river bed aggradations condition. For obtaining the bed level of the parent rock, each staff site location digging operation has been done and the depth of stone dust is measured. Deducting dust depth from present bed level, bedrock level (profile before dust deposition) is obtained for a comparable illustration of both the profiles (before and after dust deposition). While doing the depth of dust deposition, litho facets of 06 sites have also been assessed.

4.3.2.1 Methods for Assessing the Channel Path Modification Due to Direct Stone Mining from the River Bed

For assessing the impact of direct stone quarrying from river bed on river flow path we have selected some other tributaries of Dwarka river (except the previous six selected) thalweg axis of flow from 2001 to 2017 has been digitized from Google earth image and superimposed for illustrating the change. As the tributaries carry a very less amount of flow, it follows mainly the deepest part of the entire cross-section. It facilitates us to detect the thalweg axis of the concerned period easily without profiling. For making it confirm, the thalweg axis of 2017 is cross-validated with the field. The departure of the digitized thalweg axis from the field-based thalweg axis is <0.6 m in all the cases. For better visibility of the change, only two consecutive reaches of a tributary are shown here.

4.3.3 Assessing Stone Dust Accretion Susceptibility at the Riverbed

4.3.3.1 Data Layer Selection and Preparation for River Bed Accretion Susceptibility

Along with spatial stone dust accretion mapping, stone dust accretion susceptibility of two successive reaches of six selected tributaries has been done based on a multi-parametric approach. Total eleven conditioning parameters like (1) volume of dust heaping (2) direct dust deposition at the river (3) distance of river from dust heaping sites (4) distance from the crusher units (5) river bed slope (6) bed shear stress (7) velocity of flow during pre-monsoon season (8) steepness of bank slope (9) density of water (10) depth of river water (11) velocity of the river in monsoon season have been taken into account for all the selected tributaries. The digital elevation model for the mentioned parameters is prepared in Erdas software. The selection of parameters is based on the field experience and following the predecessors in this field. Jakoyljevic et al. (2009) and Mehdi et al. (2011) also studied these types of susceptibility by using few such parameters in their respective study regions.

Volume of Dust Heaping

Stone dust from the stone crusher units often influxes into the nearby river channel. The field survey was conducted to determine the dust heaping zone and the volume of dust from the distance is estimated at a surface of one square meter per location. Field experience proves that more dust is heaped to the channel near the crushing unit. On this basis, ratings 10, 7.5, 5, 2.5, and 1 are assigned to dust heaping zones, respectively, with extremely high, high, moderate, low, and very low volume. DEM is created in ERDAS remote sensing software based on the rating values of the selected sites.

Direct Dust Deposition at the River

In the present study, the authors identified direct dust deposition point (DDDP) to the river through the field visit. The area of the affected channel is demarcated by direct observation of the field. This analysis is carried out in the light of five integrated buffers from the DDDP (direct dust deposition point) and the rating is given in a specific manner. The highest rating is rated as 10 and granted to the DDDPs immediate peripheral zone (up to 250 m), rating values 7.5, 5, 2.5, and 1 are allocated to the buffer zones 250–500 m, 500–750 m, 750–1000 m and beyond 1000 m. Random points are taken from every buffer area, and every DDDP and DEM are created. Given the subjective but logical approach of assigning a weight to the buffer zone as the deposition rate decays over distance. Priority is given to deciding on buffer radius field experience and perception of people.

Distance from the Crusher Units

This analysis is also carried out considering five dispersed buffers from the units of stone crusher which are the main source of stone dust and rating is given in a specific manner. The highest rating is rated as 10 and granted to the Nearer dust deposition points (NDDP) immediate peripheral zone (up to 250 m), rating values 7.5, 5, 2.5, and 1 are allocated to the buffer zones 250–500 m, 500–750 m, 750–1000 m and beyond 1000 m. DEM is then prepared based on these values.

Bed Shear Stress

The bed shear stress (τ_0) is expressed as a force per unit area of the bed (in N m^{-2}) and increases with flow depth and channel steepness.

$$\tau = yD\mathrm{Sw} \tag{4.1}$$

where, τ = spatially averaged bed shear stress (N m^2), y = weight density of water (N m^3), D = average water depth (m), Sw = water surface slope.

It is assumed that high dust deposition offers more resistance. Forty sites in each river are selected and shear stress on those sites is computed. The river is reclassified into five rating groups, offering 10, 7.5, 5, 2.5, and 1 at very high, high, moderate, low, and very low-stress

levels, based on the range of high and low shear stress values. Based on the rating values taken randomly from different reclassified zones DEM is prepared.

Velocity of Flow During Pre-monsoon and Monsoon Season

The monsoon period and pre-monsoon period flow velocity of the river have been measured. For the selection of velocity measuring sites, random sampling rules have been followed. 40 measuring sites from each studied tributary have been selected for this study and classified into five very high to very low flow velocity zones as done in other layers and finally DEM is prepared for both the seasons.

Steepness of Bank Slope and River Bed Slope

The riverbank slope and bed slope have been measured directly from the field. The water depth and flow of the tributaries are so low that they can be measured. 40 measuring sites are selected from each tributary for this study and plotted into the ArcGIS environment. Abney level is used to measure slope. DEM is prepared based on these values. DEM is then reclassified giving a rating as given in other layers. The maximum rating of 10 is given to the lowest slope class.

Density of Water

The density according to USGS (2018) is only the weight of a specified quantity or amount of material. A common water density measurement unit is gram per milliliter (1 g ml^{-1}) or 1 g per cubic centimeter (1 g cm^{-3}). For analyzing the water density, 40 water samples from each studied tributary has been collected using the hydrometer (it is one of the most basic portable devices for scientific measurement) and classified into low to high flow water density zones as per the measured data and finally, a DEM is prepared.

Depth of River Water

Using simple staff reading depth of water is measured at 40 sites (for each tributary) from the field in post-monsoon season (Mid October to November). Based on these depth values DEM is prepared. Here it is mentioned that a lower depth of river water indicates less volume of water and less volume of water indicates the low stream energy as well as low velocity. So, the decreasing stream energy and velocity influence the probability of dust deposition on the river bed (Hofler et al. 2018; Turowski 2018). Based on this logic, reclassification of the depth layer is done and rating values are assigned. The river is reclassified into five rating classes giving 10, 7.5, 5, 2.5, and 1 at very high, high, moderate, low and very low water depth zones.

Not all parameters affect the susceptibility to dust accretion in the same direction. So for making the data layers unidirectional and standardized in the present case a ten (10) point scale of logical inference is taken into account to assign maximum point rating to a maximum chance of effect in Arc GIS software (v.10.3) by the reclassification method (Pal and Mandal 2017; Pal and Debanshi 2018). Under such a logical assumption, each parameter is categorized into ten classes, and the scale point is allocated. Figure 4.2 displays the used data layers for dust accretion susceptibility.

4.3.3.2 Susceptibility Zoning Using Fuzzy Logic

FIS is a mathematical system, which is formed by the mathematical tool of the multi-value logic base. Zadeh (1965) introduced the theory of fuzzy set and has since been widely used to develop complicated models in various fields.

A fuzzy logic system simulates the whole system to delineate the notion out of inputs spatial data layers of the model. The Mamdani method (Yanar 2003) is the greatest used FIS. This Mamdani method attempts higher performance to appraise people's know-how and factual involvement in classification as well as accountability (Mamdani 1977). This system mainly constitutes four stages (Sami et al. 2014) namely—(i) fuzzification of the data set (ii) evaluation of the rule (iii) inference of the product of fuzzy (iv) operations of the de-fuzzification.

The entire model was accomplished in the ArcGIS environment by applying two tangible tools—(i) membership fuzzy tool (ii) fuzzy

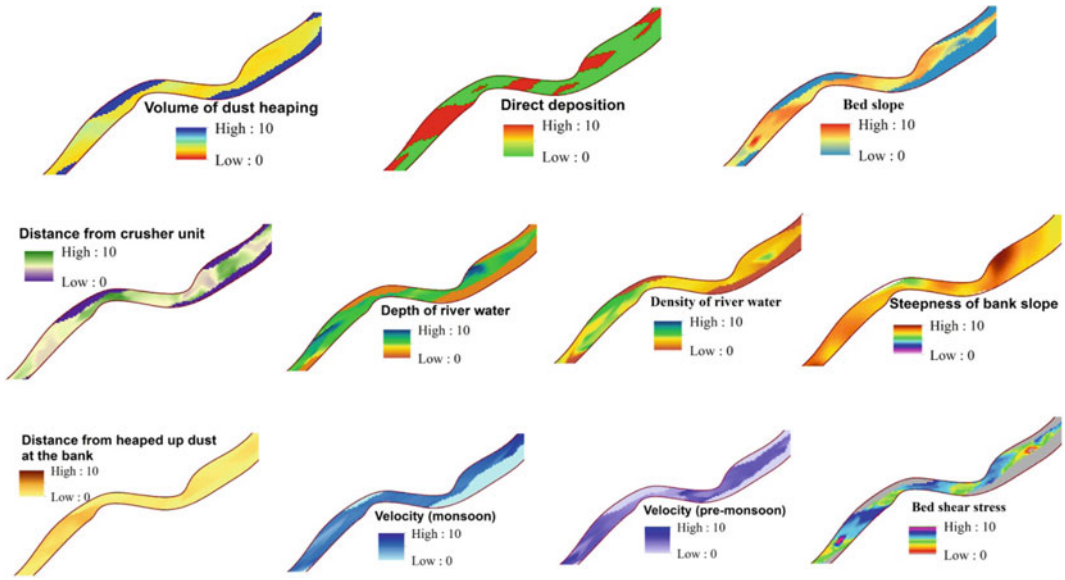

Fig. 4.2 Spatial data layers of the selected tributary 6 (Segment I) for the river bed accretion susceptibility model

overlay tool. First, all data are transformed into fuzzy and subsequently categorized into four categories which, according to the expert judgment, demonstrate high vulnerability to low. Therefore, we used a large membership operation with the help of Eq. 4.2 in the context of a few continuing membership functions.

The large membership function is used to indicate the fact that large values of the input raster have high membership in the fuzzy set.

$$\mu(x) = \frac{1}{1 + \left(\frac{x}{f_j}\right)^{-f_i}} \tag{4.2}$$

where, $\mu(x)$ = fuzzy membership function, f_i = spread (default is 5 in ArcGIS environment for large membership) f_j = midpoint of the range of values, x = degree of a element. The membership value of each component indicates a different degree of support and confidence from 0 to 1 according to this approach (Ercanoglu and Gokceoglu 2002). In Eq. 4.3, the fuzzy set is formulated.

$$a = \{x(fx)\} \tag{4.3}$$

where, a = fuzzy set, x = membership value of the elements, fx = fuzzy membership function.

In this study, the fuzzy 'if–then' method is formulated to make the zonations of river bed accretion susceptibility. The susceptibility maps are categorized into several zones (very high, high, moderate, and low) to explicit the spatial variability of that vulnerability. The following logical structure defines the fuzzy rules, i.e., If the average volume of dust heaping is high or direct dust deposition at the river is high or distance of river from dust heaping sites is less or distance from the crusher units is less or river bed slope is low or bed shear stress is high or velocity of flow during pre-monsoon season is low or steepness of bank slope is high or density of water is high or depth of river water is low and velocity of the river in monsoon season is low then river bed accretion susceptibility will be high.

4.3.3.3 Methods for River Bed Accretion Susceptibility Model Using Random Forest Algorithms (RFA)

The RFA is one of the more versatile data classification algorithms and it can classify a large volume of data using numerous attributes. The algorithm itself is very well suited to parallelization the RAF consists of different attributes.

This is a supervised method of machine learning for classification and regression analysis (Breiman 2001; Youssef et al. 2016; Naghibi et al. 2017; Gayen et al. 2019). A decision tree has to be developed to get the class output and obtain the dependent variable, respectively to classification and regression of the data sets (Kim et al. 2018). This approach consists of several decision trees and integrates them to clarify the spatial connection between the vulnerability of the river bed and the factors of stone dust affecting it (Kim et al. 2018). The advantages of the RFA model in comparison to other methods are (1) it can handle large datasets with high dimensionality as well as avoid the overfitting of the datasets. (2) No assumptions on explanatory and response variables are necessary and (3) it does not require any prior data to transform and rescale the datasets (Youssef et al. 2016; Naghibi et al. 2017). The vector of prediction is indicated with log $2(M + 1)$, where M indicates the algorithm input number (Kim et al. 2018). Mean squared error can be estimated to test the model's output (Kim et al. 2018).

$$\varepsilon = (V_{\text{observed}} - V_{\text{response}})^2 \tag{4.4}$$

where ε represents the mean-square error, V_{observed} is the observed data, and V_{response} indicates the variable's outcome.

RF is used to regulate the division in every node by the number of trees and the numbers of predictive variables (Naghibi et al. 2017). The average tree projection is estimated as

$$S = \frac{1}{k} \sum k^{\text{th}} v^{\text{response}} \tag{4.5}$$

where S marks every forecast of forest and K reflects the trees of the model.

This study moved forward using the four key measures: (1) first preparation and collection of the dataset of river bed accretion susceptibility. Regarding this work, eleven predisposing factors were considered. (2) Preparing data sets for testing and validation by repeated random sampling. (3) River bed accretion susceptibility mapping using RF machine learning algorithm. (4) Finally, validation of the model by the remaining validation datasets. This RF model was implemented in R (version 3.2.4) software using the "randomForest" package. For an RBAS, data representing both sensitive and non-sensitive areas are the main requirements. Conditioning data is typically stored as ArcGIS grid cell layers. The outcome of the decision trees was generated based on the RF model. Finally, the spatial model output was transferred into ArcGIS and reassess into four classes namely high, moderate, low, and very low river bed accretion susceptibility based on natural break statistics. The accuracy of the models was tested. The overall training datasets are usually split by 70% of the samples for training models and others for validation.

Assessing Performance of the Models

A total of 32 field sites from each tributary are visited for measuring the depth of dust accretion over the river bed. Based on these field and model data, Kappa coefficient, area under the curve in Receiver Operating Curve, and correlation coefficient are computed.

For validating the prepared river bed accretion susceptibility models receiver operating characteristics (ROC) curve is prepared. That is invented to appear in the true positive rate (TPR) in respect of false-positive rate (FPR) at assorted threshold contexts. The AUC is known as the fitness rate. It helps to compute the succession and prediction rate. Rasyid et al. (2016) categorized this area under curve into five classes such as (i) excellent (0.90–1.00), (ii) good (0.80–0.90), (iii) satisfactory (0.70–0.80), (iv) poor (0.60–0.70) and (v) fail (0.50–0.60). SPSS statistics software (v.17.0) has been used for preparing the ROC curve as well as the success and prediction rates.

Kappa coefficient (Eq. 4.6) and Overall accuracy (Eq. 4.7) assessment also have been carried out for the derived accretion susceptibility models. Kappa coefficient values range from 0 to 1. As per the recommendation of Monserud and Leemans (1992) that Kappa coefficient values ranges <0.4 represent the poor or very poor agreement, 0.4–0.55 represent the fair agreement, 0.55–0.7 represents good agreement and the 0.7–

0.85 agreement is very good and the >0.85 agreement between models and the ground reality is outstanding.

$$k = \frac{N\sum_{i-1}^{r} Xii - \sum_{i-1}^{r}(xi + {}^{*}xi + i)}{N^2 - \sum_{i-1}^{r}(xi + {}^{*}xi + i)} \quad (4.6)$$

where N refers to overall pixel count; r refers to matrix number of rows; Xii equal to the number of rows i observation and columns ii, xi and $x + i$ = marginal totals for both the row.

$$\text{Oac} = \text{Tncs}/100\% \text{ of Tsm} \quad (4.7)$$

where Oac = Overall accuracy, Tncs = complete valid sample number, Tsm = Total sample.

4.3.4 Measuring Sediment Load

Suspended and soluble sediment load is measured at all six selected tributaries. All the cases measuring temporary stations are at the confluence point of the tributaries. The suspended load is measured at different discharge levels and based on these data; the suspended sediment load rating curve is prepared following power regression Eq. 4.8. A rating curve is plotted over a log–log graph. The power regression equation and coefficient of determination can state the direction and degree of change of sediment load in about change of discharge.

$$\begin{aligned} \log_{10} F(x) &= m \log_{10} x + b \\ F(x) &= x^m.10^b \end{aligned} \quad (4.8)$$

where m is the slope; b is the intercept point on the log plot; x = log$x$ and y = log$y$.

4.3.5 Methods for Analyzing Water Quality

40 water samples from various Dwarka river affluents were obtained in different stone mining areas to examine water quality. Physico-chemical properties of water (referred to in Table 4.3) have been tested and the results are compared to the standard state of water quality as defined by BIS (1991) and ISDW (1963). Some water sample parameters such as actual water temperature, pH, and watercolor are gradually measured on-site after water sample collection with the digital thermometer, pH meter, and visual espial. The water sample was collected in glass bottles to analyze the dissolved oxygen and then added dissolved oxygen reagents. We used the azide modification method for the Winkler method here (The technique of azide modification is a standard method for testing the DO). The laboratory test method is used to test the chemical oxygen demand (COD), alkalinity, and total hardness (Th) for analysis. To analyze selected parameters that exceed the threshold limit after Ramesh et al. (2008) we have applied the parameter specified water quality index (PSWQI) with certain necessary modifications. The individual quality ratings (IQRs) of BOD, COD, DO and TDS based on Eq. 4.9 have been done for better understanding.

$$\text{PSWQI} = 100(\text{Vi}/\text{Si}) \quad (4.9)$$

where PSWQI = the selected specific parameter's sub-index, Vi = the tested value of the parameter, Si = standard value.

4.4 Results

4.4.1 Volume of Dust Deposition

Table 4.1 depicts the volume of dust deposition in the selected six tributaries at eight sample sites. The volume of dust differs from 302 to 978 kg m^{-3} in the case of all the tributaries. The mean value varies from 601 to 759 kg m^{-3} and its variation is mainly determined by the nearness of stone crushing units, their total dust production, the velocity of water, etc. Tributary 4 registered maximum dust deposition in its course owing to 489–987 kg m^{-3}.

4.4.2 Channel Bed Accretion

Due to the seasonal rainfall and scanty runoff at the source segment tributaries, stone dust often

becomes consolidated over the river bed and pond. Stone dust is often deposited over the river bed and pond due to seasonal rainfall and insufficient drainage in the source segment tributaries. The depth of stone dust varies from 0.02 to 0.52 m according to the January 2018 measurement (Fig. 4.3a–f). At the proximity of the stone crusher units, the dust depth is maximal. The amount of inflow of stone dust to the tributaries is high during the monsoon season due to maximum surface runoff triggered by high rainfall concentration. The average suspended load during the monsoon period is 15,762 g m^{-3}. Due to the rise of discharge during monsoon, a good amount of loose dust is discharged further downstream. A lot of loose dust is released further downstream due to the increase of discharge through monsoons. But such dust heaped the armoring of the river's bed during the non-monsoon seasons.

Field observation of the litho facets (avg. condition) (Fig. 4.4) This difference in composition and their varying width can be explained in terms of size of the produced stone chips, influencing factors of dust deposition in the river bed, and so on.

4.4.3 Simulated Result of River Bed Accretion Susceptibility and Performance Assessment

Figures 4.5 and 4.6, respectively illustrate river bed accretion susceptibility model in selected two reaches of each six tributaries using Fuzzy inference system (FIS) and Random Forest Algorithm (RFA) compiling eleven conditioning parameters. In the case of FIS and RFA very high accretion susceptible zone covers from 5 to 12% in the former model and 4–21% in the case of the latter model. Tributary 5 and 4 have appeared as the most susceptible as per both the applied models. Flowing of those rivers across highly dense crusher units strongly influences such high susceptibility. Figure 4.6 also displays which factor is dominantly responsible for accretion susceptibility. Direct deposition of dust at the river bed, the distance of river from heaped up dust site, distance from crusher unit, bed slope are some dominant conditioning factors for susceptibility.

Table 4.2 shows the estimated *K*, AUC, and *r* values of two used models in all the tributaries. *K* value ranges from 0.81 to 0.93 which means that the relationship between model state and ground reality is good to excellent. While justifying the applicability and interpretability of the applied two models, it can be stated that RFA is more effective in these cases as the average *K* value (0.91) shows good agreement on the FIS model between model and ground reality (Mean $K = 0.84$). AUC values (>0.8) are also acceptable for both the models but the RFA model (0.9) shows better agreement than the FIS model (0.84). The correlation coefficient between the depth of deposition and model value ranges from 0.71 to 0.82. At the 0.01 confidence level, all of these values are significant. However, the degree of correlation is high in the case of the RFA model.

Table 4.1 Tributary and site-specific volume of dust estimation (kg m^{-3})

Tributary	Volume of dust (kg m^{-3})							
	Site 1	Site 2	Site 3	Site 4	Site 5	Site 6	Site 7	Site 8
Tributary 1 (T_1)	487	964	784	978	648	324	321	302
Tributary 2 (T_2)	845	479	487	475	815	426	654	654
Tributary 3 (T_3)	968	475	963	364	785	463	427	472
Tributary 4 (T_4)	489	889	785	987	624	745	752	804
Tributary 5 (T_5)	897	876	396	874	785	354	365	904
Tributary 6 (T_6)	879	635	478	587	745	748	742	421

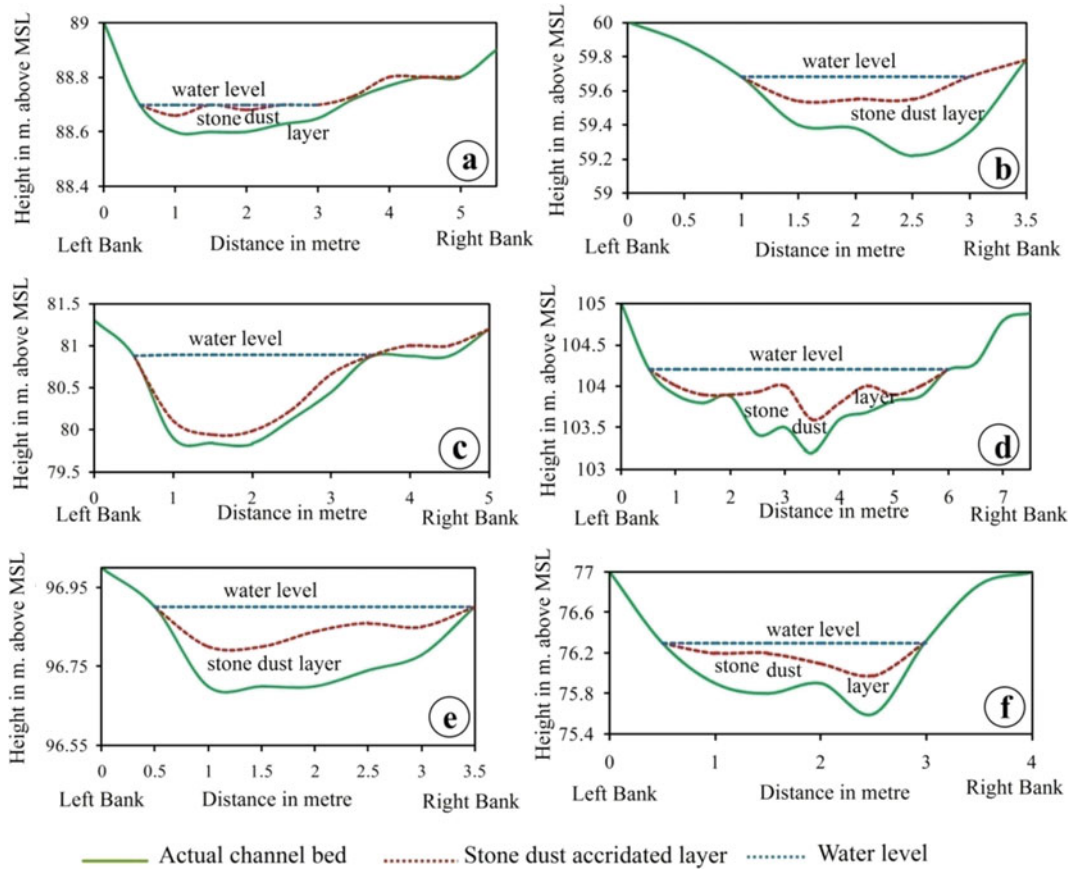

Fig. 4.3 Cross-sections of the selected tributaries (**a**–**f**), showing the current level of channel bed accredited with stone dust

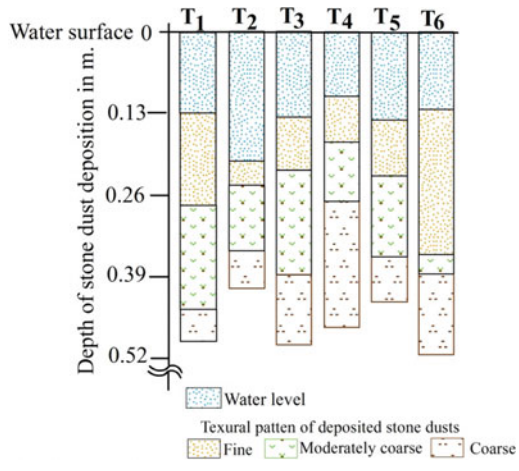

Fig. 4.4 Litho facets of the river bed deposition

4.4.4 Shifting of Flow Paths

Figures 4.7 and 4.8 display the thalweg shifting of a tributary from 2001 to 2017. There is no definite trend of shift due to irregular mining of stone from the river bed. The average yearly shifting is 42 m. Some parts of the selected reaches show a very high rate of annual shifting (>85 m). It mainly depends on where good quality of the stone is found. On a riverbank where there is a good quality of stone for the concerned mining, shifting tendency is toward that side. It causes asymmetric channels and increases the chance of riverbank failure (Das et al. 2013). The average depth of mining in all six tributaries varies from 10 to 80 cm.

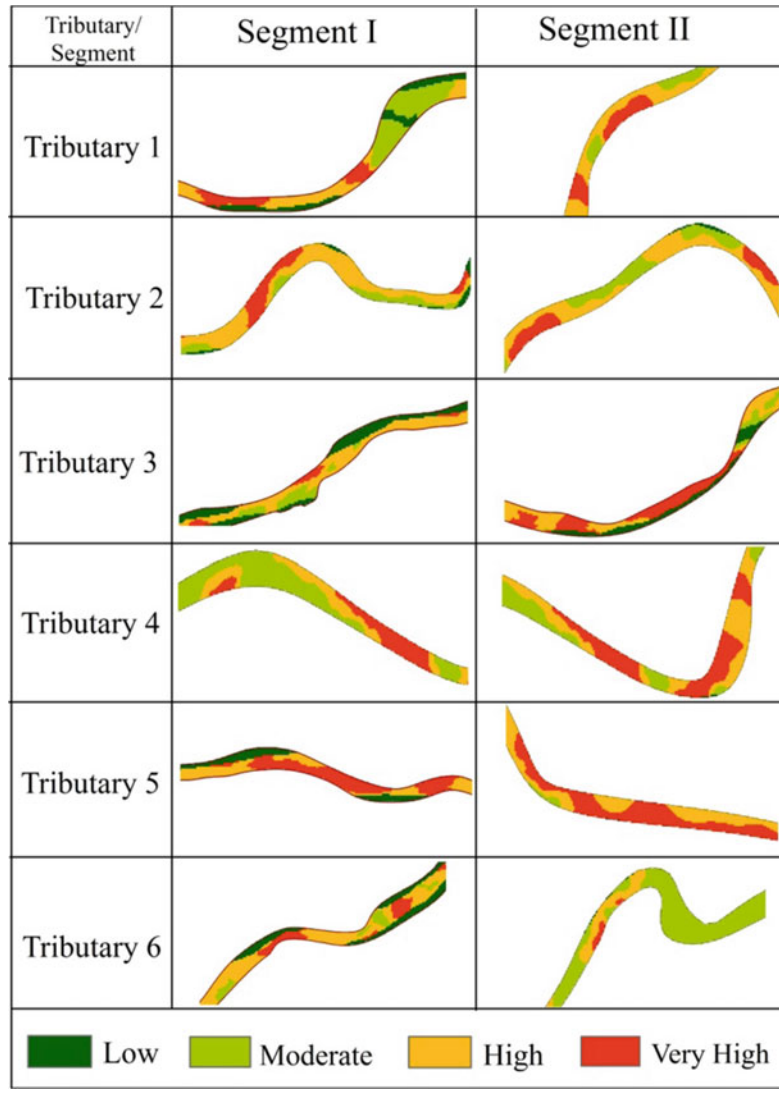

Fig. 4.5 River bed accretion susceptibility (RBAS) model using fuzzy inference system (FIS)

Interestingly, the small-scale mining of stone for grinder, stone pots, statues, etc. causes the formation of small geometric pothole-like features over the river bed. It also causes increasing turbulence in the river flow.

4.4.5 Impact on Sediment Flow

Sediment load in the rivers of the Rarh region is recorded high in most cases. But it is rather high in the areas with the thermal plant producing huge fly ash, stone mining, and crushing units (Pal and Mandal 2019a, b). Such a difference is registered when sediment load is compared with rivers affected by stone dust and free from such a problem. Figure 4.9 depicts the suspended sediment load rating curve describing the influence of discharge on load. The volume of load ranges from 6584 to 79,888 g m^{-3} with a discharge of 1–25.5 m^3 s^{-1} in all six selected affected tributaries. The mean sediment load of the rivers ranges from 7420 to 31,245 g m^{-3}. The highest sediment load is recorded in the tributaries flowing across densely settled crusher units. The composition of load depicts that out of total load >75% is stone dust. While describing the relation between discharge and sediment load, most

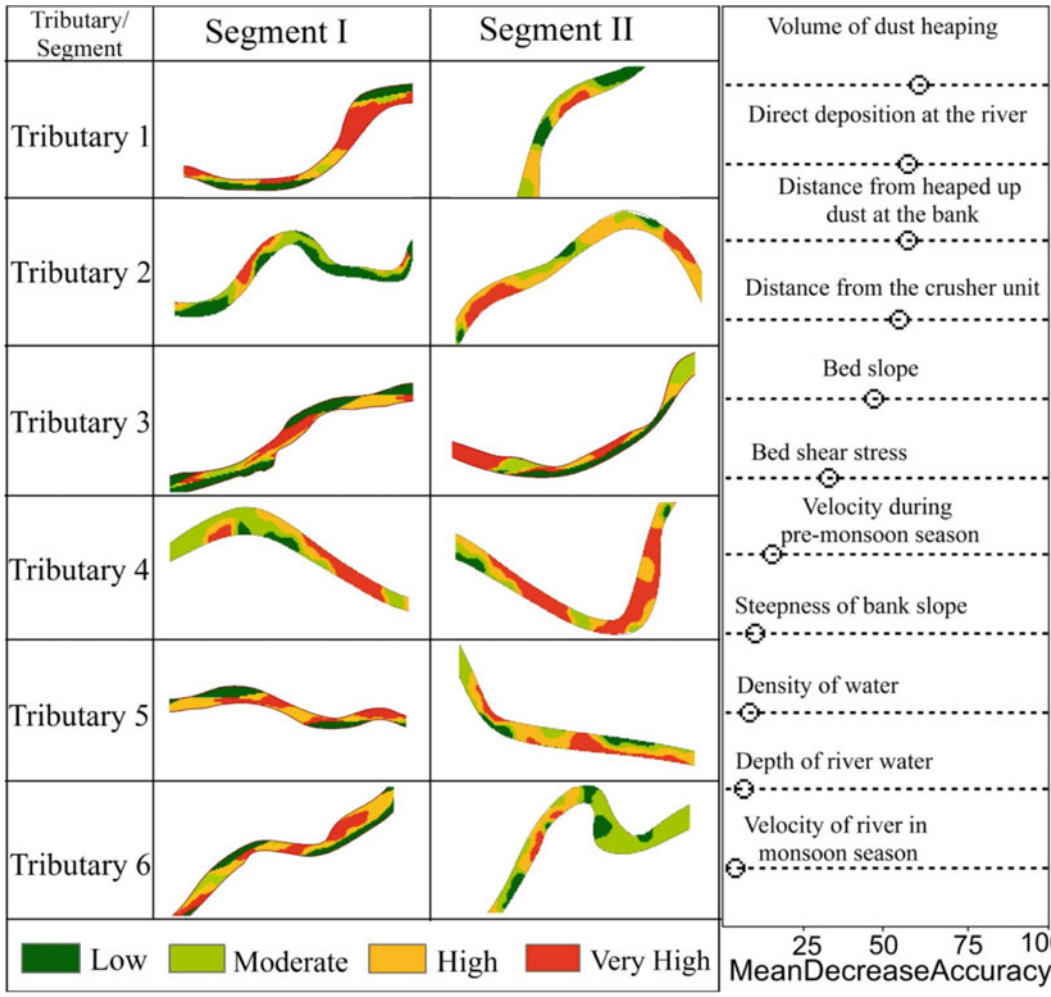

Fig. 4.6 River bed accretion susceptibility (RBAS) model using the random forest algorithm

Table 4.2 Performance level of the applied models for accretion susceptibility

Error estimation	Model	T_1	T_2	T_3	T_4	T_5	T_6
Kappa coefficient	FIS	0.89	0.81	0.92	0.84	0.81	0.82
	RFA	0.92	0.91	0.9	0.89	0.94	0.93
AUC value	FIS	0.821	0.806	0.802	0.874	0.852	0.866
	RFA	0.922	0.905	0.879	0.887	0.912	0.886
Correlation coefficient	FIS						
	RFA	0.745	0.82	0.745	0.654	0.712	0.802

of the tributaries recorded breakpoints indicating decreasing carrying capacity and thus deposition of sediment over the river bed. From the regression graphs for each tributary (Fig. 4.9), it is observed that trend is positive and the coefficient of determination (R^2) value is 0.6–0.75 with a p-value < 0.05. These statistics demonstrate the controlling power of discharge

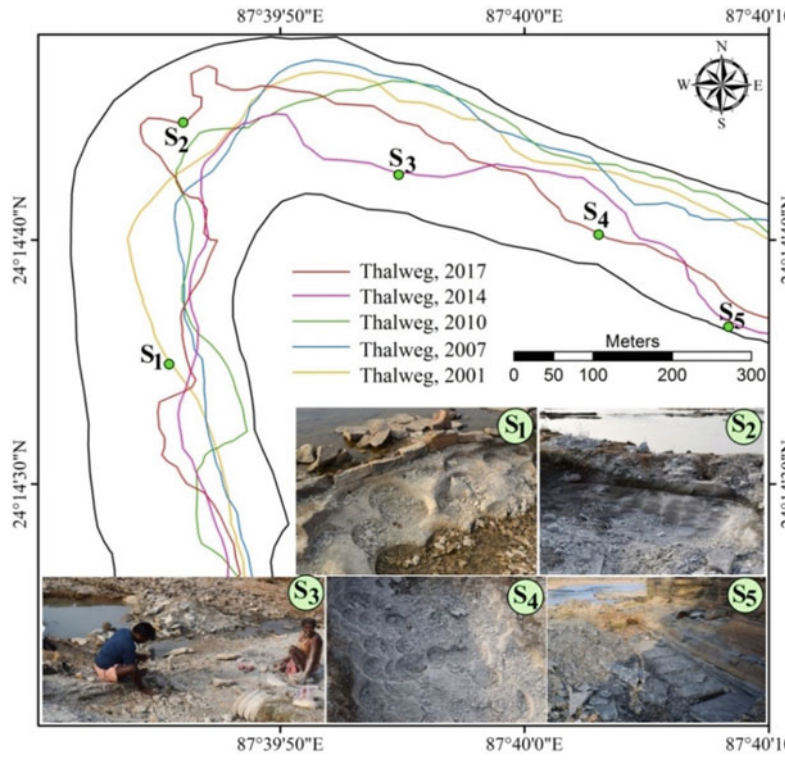

Fig. 4.7 Shifting of thalweg lines (2001–2017) (Reach 1)

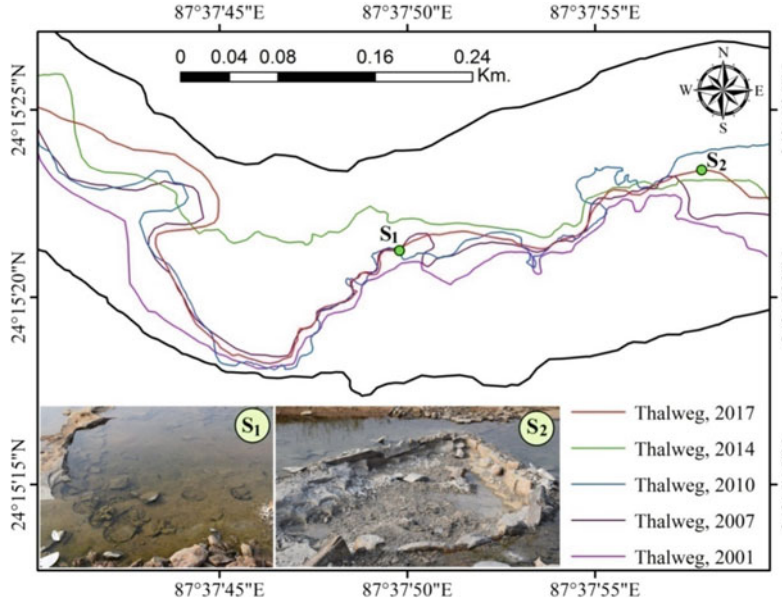

Fig. 4.8 Shifting of thalweg lines (2001–2017) (Reach 2)

on sediment load is significant but not absolute. If the R^2 value would be near 1 or 1 it could be stated that discharge is the absolute determinant of sediment load. But as the computed value is not 1, the influences of other factors could be anticipated.

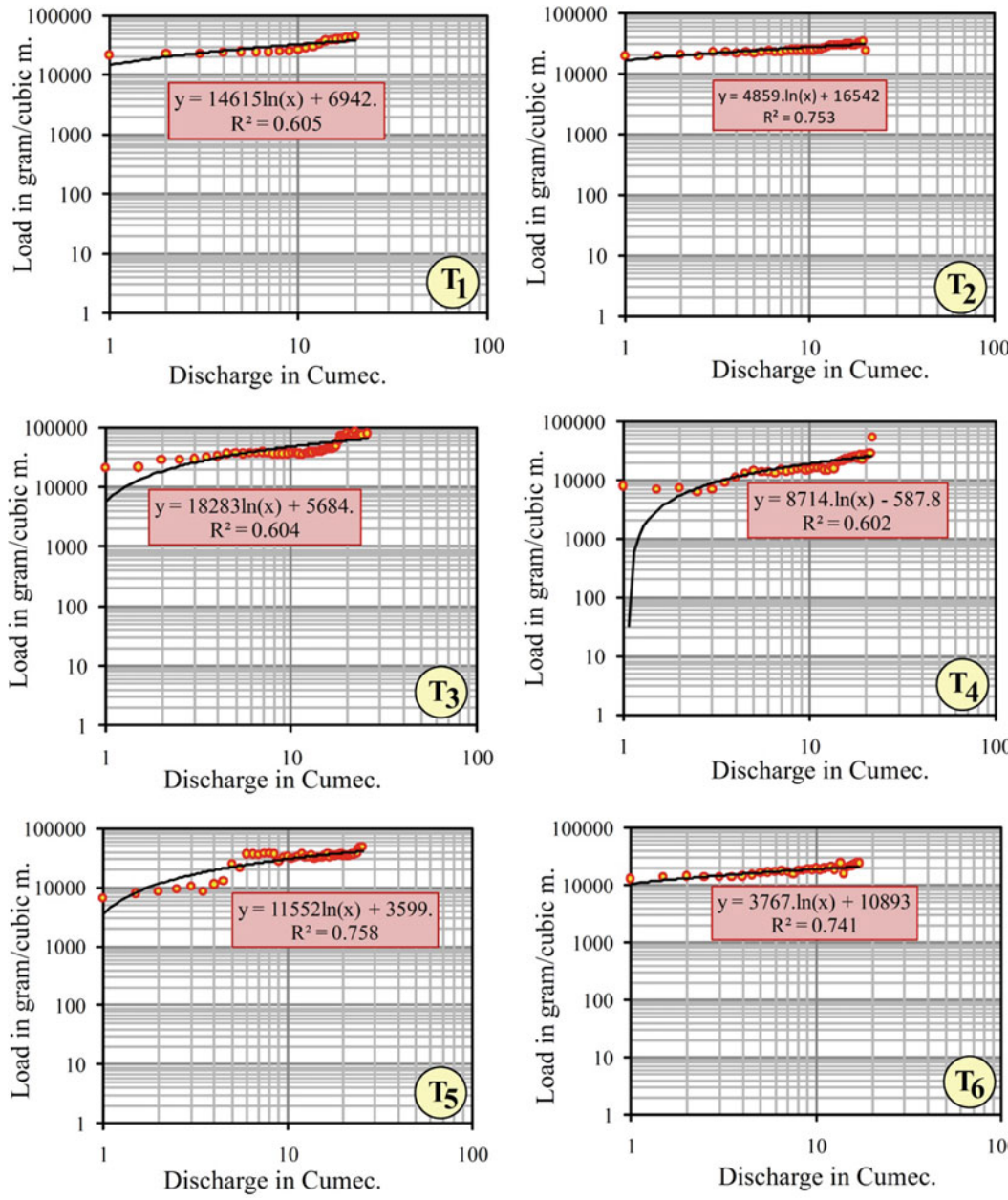

Fig. 4.9 Suspended and dissolved sediment load—(T_1) for selected tributary 1, (T_2) for tributary 2, (T_3) for the selected tributary 3, (T_4) for tributary 4, (T_5) for tributary 5, and (T_6) for the studied tributary 6

4.4.6 Impact on Ambient Water Quality

Table 4.3 shows that the selected tributaries' average water quality condition exceeds the permissible drinking and irrigation threshold set by BIS (1991). For example, the allowable pH for drinkable water is between 6.5 and 8.5 and for irrigation is 6–8.5 but for three tributaries it is observed that pH is >8.5. In all cases, BOD and COD excessively exceed the permissible limit (Table 4.3). Excessive water BOD means that the

Table 4.3 Tributary wise water quality status (physico-chemical properties) with standard permissible limits (BIS 1991)

Physico-chemical parameters	Selected tributaries						
	Tributary 1 (T_1)	Tributary 2 (T_2)	Tributary 3 (T_3)	Tributary 4 (T_4)	Tributary 5 (T_5)	Tributary 6 (T_6)	Standard permissible limit (mg/L)
PH	8.1	8.9	8.4	8.8	8.1	8.6	6.5–8.5
DO (ppm)	3.11	3.23	2.98	2.99	2.89	3.17	4.0–6.0
TDS (mg/l)	2344	2421	2398	2414	2143	1948	500
COD (mg/l)	12,745.4	13,149.4	12,632.8	12,879.4	12,360.8	12,543.2	10
BOD (mg/l)	41.6	47.8	30.3	41.3	35.7	41.8	3
Transparency (cm)	3.7	4.4	4.1	5.9	4.9	5.7	–

river and pond water are oxygen-deficient and that there is an aerobic condition there. The development of aquatic life is very detrimental to this situation. This prevents the cycle of decomposition of organic waste. The total dissolved solids (TDS) measured in the water for all levels are 4–5 times the normal level for the water quality. Water quality is 9–16 times higher in cases of biological oxygen demand (BOD) and chemical oxygen demand (COD) is 1308–1378 times enhanced than the standard limit.

4.5 Discussion

Stone crusher units specifically produce micro stone chips that can yield more dust. Micro-level stone dust particles spread over the larger part of the surrounding crusher center. According to the central pollution control board of India (CPCB 2009), the real dust production area is fairly small it is about 0.5–1 m^2. But the dust spreads more than 10–15 times larger and definite emission at near about 3–8 m height. Stone dust admixing to the surrounding river water contaminates the water quality (Singh et al. 2016; Okafor and Egbe 2017; Van Duc and Kennedy 2018; Pal and Mandal 2019a, b). The excessive influx of dust can change the river morphology as found in the present case. Increasing sediment load, and river bed aggradations are the direct footprint observed in the tributaries of the Dwarka River basin. Tributaries flowing across densely located crusher units are more affected by this problem. As most of the tributaries carry very scant water or remain dry during the non-monsoon period, rivers get the ambiance of dust deposition (Faershtein et al. 2016; Pal and Mandal 2017, 2019a, b). Moreover, during monsoon time discharge level of the river is not so high to carry out all the dust deposited over the river bed. Moreover, during this time a huge amount of dust was additionally admixed into the river through surface runoff. So, dust remainder within the river is a very common fact and it causes the change in river morphology (Mugade and Sapkale 2015; Ali et al. 2017). If gradually the rivers lose their carrying capacity in this way in future dust may affect wider surfaces specifically agricultural land. Analysis of river bed accretion susceptibility can give a picture of susceptible areas of dust deposition. An advanced simulation model with acceptable accuracy can guide what measures could be taken where for discharging stone dust for the sustenance of the river. Direct mining of stone from river beds creates manmade micro-level pools over there which changes the flow resistance and flow characters (Padmalal et al. 2008; Sreebha and Padmalal 2011; Preciso et al. 2012; Brunier et al. 2014; Wang et al. 2018). The laminar character of flow in most of the cases has converted into the turbulent flow (Lajeunesse et al. 2010; Martín-Vide et al. 2010; Bhuiyan et al. 2014). Excessive sediment load contributed from crusher units is majorly responsible for

aggradation of river bed and change of channel morphology. Original bed topography is armored with thick stone dust. People harvest stone from the river bed in a very irregular manner based on the quality of stone and accessibility of harvesting (Padmalal et al. 2008; Kamboj et al. 2017; Sadeghi et al. 2018; Ciszewski 2019). It controls the flow path of the river. Sometimes mining from riverside is caused for riverbank failure and severe change of thalweg line. In this thalweg, a shift is given priority since river bed mining is concerned (Omoti et al. 2016; Kamboj and Kamboj 2019). Overall river shifting is not so high in the studied segment. Mossa and James (2013) reported river shifting due to stone and sand mining from river bed and soil from the river bank. It often causes loss of agricultural land settlement areas. The present study area is sparsely settled and there is very little chance of engulfing the settlement area.

Water quality change is another major concern as reported in the present study area. The enhanced degree of BOD, COD, turbidity level, and PH all can adversely affect the habitat quality of the river and species diversity and safety (Mandal and Pal 2021). Armoring river bed with stone dust creates an artificial habitat platform where species have to be re-adapted. It strongly hampers the functionalities of the primary produces (Ashraf et al. 2011; Monjezi et al. 2013; Brunier et al. 2014; Mudenda 2018). Pal et al. (2016) identified the lowering rate of fish production and breaching of some fish species. Increasing turbidity level can influence to enhance the temperature of the water which withstands against the growth of species.

Fly ash and stone dust-induced water quality change is a very common issue addressed by many scholars (Saha and Padhy 2011; Divya et al. 2012; Ozcan et al. 2012; Pal et al. 2016; Pal and Mandal 2017). But the change of river morphology like the change of sediment load, simulation models for identifying river bed accretion sites due to stone dust deposition, and shifting of thalweg due to river bed mining are some new dimensions of this work.

Few limitations of this work could be pointed out. Gauge data relating to discharge and load for a long time across different rivers can provide a strong database for analysis. Instead of only six tributaries as sample study, more number of samples from different mining and crushing landscape could provide a more comprehensive result.

4.6 Conclusions

Stone dust is often a major cause of channel bed accretion in the tributaries of the river flowing across stone quarrying and crushing units. Admixing of dust in water is responsible for increasing sediment load in water and, when it is beyond carrying capacity, it precipitates in the river bed. Assessing potential areas susceptible to dust accretion in rivers identified 6–17% areas, which represent very high susceptible zones. Direct riverbed stone mining for small-scale industries is caused for frequent diversion of the flow axis of the rivers. River water contamination due to stone dust is well identified and the level of contamination is often beyond irrigability and drinkability. Moreover, such contamination may also affect the normal ecological functioning of river water. The continuous deposition may convert the small tributaries or parts of it into the land. These examples denote the change in fluvio-geomorphic setup of the river. Considering the serviceability of the river, crusher units should be more cautious about discharging stone dust. The ancillary dust refinery industry may solve this problem to some extent as the refine dust may be used for some other industries like fertilizer, cement, etc.

Funding NA.

Conflict of Interest None.

References

Affandi FA, Ishak MY (2019) Impacts of suspended sediment and metal pollution from mining activities on riverine fish population—a review. Environ Sci Pollut Res 1–13

Ali ANA, Ariffin J, Razi MAM, Jazuri A (2017) Environmental degradation: a review on the potential impact of river morphology. In: MATEC web of conferences, vol 103, p 04001

Ashraf MA, Maah MJ, Yusoff I, Wajid A, Mahmood K (2011) Sand mining effects, causes and concerns: a case study from Bestari Jaya, Selangor, Peninsular Malaysia. Sci Res Essays 6(6):1216–1231

Barman B, Kumar B, Sarma AK (2018) Turbulent flow structures and geomorphic characteristics of a mining affected alluvial channel. Earth Surf Proc Land 43 (9):1811–1824

Bhuiyan AA, Amin MR, Karim R, Islam AKMS (2014) Plate fin and tube heat exchanger modeling: effects of performance parameters for turbulent flow regime. Int J Autom Mech Eng 9(1):1768–1781

BIS (1991) Indian standard drinking water-specification. Bureau of Indian Standard, New Delhi. Accessed Sept 2016. https://law.resource.org/pub/in/bis/S06/is.10500.1991.pdf

Breiman L (2001) Random forests. Mach Learn 45(1):5–32

Brunier G, Anthony EJ, Goichot M, Provansal M, Dussouillez P (2014) Recent morphological changes in the Mekong and Bassac river channels, Mekong delta: the marked impact of river-bed mining and implications for delta destabilisation. Geomorphology 224:177–191

Calle M, Alho P, Benito G (2017) Channel dynamics and geomorphic resilience in an ephemeral Mediterranean river affected by gravel mining. Geomorphology 285:333–346

Chen J, Li K, Chang KJ, Sofia G, Tarolli P (2015) Open-pit mining geomorphic feature characterisation. Int J Appl Earth Obs Geoinf 42:76–86

Ciszewski D (2019) The past and prognosis of mining cessation impact on river sediment pollution. J Soils Sediments 19(1):393–402

Costea M (2018) Impact of floodplain gravel mining on landforms and processes: a study case in Orlat gravel pit (Romania). Environ Earth Sci 77(4):119

CPCB (2009) Comprehensive industry document stone crushers. Central Pollution Control Board, Government of India. Series: COINDS/78/2007-08, 1.1–8.21, www.cpcb.nic.in

Das P, Let S, Pal S (2013) Use of asymmetry indices and stability indices for assessing channel dynamics: a study on Kuya river, eastern India. J Eng Comput Appl Sci 2(1):24–31

Dembowska EA, Mieszczankin T, Napiórkowski P (2018) Changes of the phytoplankton community as symptoms of deterioration of water quality in a shallow lake. Environ Monit Assess 190(2):95

Divya CM, Divya S, Ratheesh K, Volga R (2012) Environmental issues in stone crushers. Pudong, Shanghai, China. Accessed 2016 Aug 15. https://businessimpactenvironment.wordpress.com/2012/01/08/environmental-issues-in-stonecrushers/

Ercanoglu M, Gokceoglu C (2002) Assessment of landslide susceptibility for a landslide-prone area (north of Yenice, NW Turkey) by fuzzy approach. Environ Geol 41(6):720–730

Esposito G, Mastrorocco G, Salvini R, Oliveti M, Starita P (2017) Application of UAV photogrammetry for the multi-temporal estimation of surface extent and volumetric excavation in the Sa Pigada Bianca open-pit mine, Sardinia, Italy. Environ Earth Sci 76(3):103

Faershtein G, Porat N, Avni Y, Matmon A (2016) Aggradation–incision transition in arid environments at the end of the Pleistocene: an example from the Negev Highlands, southern Israel. Geomorphology 253:289–304

Festin ES, Tigabu M, Chileshe MN, Syampungani S, Odén PC (2019) Progresses in restoration of post-mining landscape in Africa. J For Res 30(2):381–396

Fu X, Wang SX, Cheng Z, Xing J, Zhao B, Wang JD, Hao JM (2014) Source, transport and impacts of a heavy dust event in the Yangtze River Delta, China, in 2011. Atmos Chem Phys 14(3):1239–1254

Fu X, Cheng Z, Wang S, Hua Y, Xing J, Hao J (2016) Local and regional contributions to fine particle pollution in winter of the Yangtze River Delta, China. Aerosol Air Qual Res 16:1067–1080

Gayen A, Pourghasemi HR, Saha S, Keesstra S, Bai S (2019) Gully erosion susceptibility assessment and management of hazard-prone areas in India using different machine learning algorithms. Sci Total Environ 668:124–138

Hauer C, Schober B, Habersack H (2013) Impact analysis of river morphology and roughness variability on hydropeaking based on numerical modelling. Hydrol Process 27(15):2209–2224

Hofler S, Piberhofer B, Gumpinger C, Hauer C (2018) Status, sources, and composition of fine sediments in upper Austrian streams. J Appl Water Eng Res 6 (4):283-297

Hohensinner S, Hauer C, Muhar S (2018) River morphology, channelization, and habitat restoration. In: Riverine ecosystem management. Springer, Cham, pp 41–65

Holmes RM, Mc Clelland JW, Peterson BJ, Tank SE, Bulygina E, Eglinton TI, Staples R (2012) Seasonal and annual fluxes of nutrients and organic matter from large rivers to the Arctic Ocean and surrounding seas. Estuaries Coasts 35(2):369–382

https://www.cpcb.nic.in/National_Air_Quality_Standards.php.

ISDW (1963) Indian standard methods of test for aggregates for concrete IS: 2386 (Part III). Bureau of Indian Standards

Jakovljevic B, Paunovic K, Belojevic G (2009) Road-traffic noise and factors influencing noise annoyance in an urban population. Environ Int 35:552–556. https://doi.org/10.1016/j.envint.2008.10.001

Jha VC, Kapat S (2009) Rill and gully erosion risk of lateritic terrain in South-Western Birbhum District, West Bengal, India. J Eng Comput Appl Sci 2(1):24–31

Kamboj N, Kamboj V (2019) Riverbed mining as a threat to in-stream agricultural flood-plain and biodiversity of Ganges River, India

Kamboj V, Kamboj N, Sharma S (2017) Environmental impact of river bed mining—a review. Int J Sci Res Rev 7(1):504–519

Khalid S, Shahid M, Bibi I, Sarwar T, Shah A, Niazi N (2018) A review of environmental contamination and health risk assessment of wastewater use for crop irrigation with a focus on low and high-income countries. Int J Environ Res Public Health 15(5):895

Kim JC, Lee S, Jung HS, Lee S (2018) Landslide susceptibility mapping using random forest and boosted tree models in Pyeong-Chang, Korea. Geocarto Int 33(9):1000–1015

Lajeunesse E, Malverti L, Charru F (2010) Bed load transport in turbulent flow at the grain scale: experiments and modeling. J Geophys Res Earth Surf 115 (F4)

Lei K, Pan H, Lin C (2016) A landscape approach towards ecological restoration and sustainable development of mining areas. Ecol Eng 90:320–325

Lyons C, Carothers C, Reedy K (2016) Means, meanings, and contexts: a framework for integrating detailed ethnographic data into assessments of fishing community vulnerability. Mar Policy 74:341–350

Mamdani EH (1977) Application of fuzzy logic to approximate reasoning using linguistic synthesis. IEEE Trans Comput 26(12):1182–1191

Mandal I, Pal S (2020) COVID-19 pandemic persuaded lockdown effects on environment over stone quarrying and crushing areas. Sci Total Environ 732:139281

Mandal I, Pal S (2021) Assessing the impact of ecological insecurity on ecosystem service value in stone quarrying and crushing dominated areas. Environ Devel Sustain pp 1–25

Mariya A, Kumar C, Masood M, Kumar N (2019) The pristine nature of river Ganges: its qualitative deterioration and suggestive restoration strategies. Environ Monit Assess 191(9):542

Martín-Vide JP, Ferrer-Boix C, Ollero A (2010) Incision due to gravel mining: modeling a case study from the Gállego River, Spain. Geomorphology 117(3–4):261–271

Massi L, Maselli F, Rossano C, Gambineri S, Chatzinikolaou E, Dailianis T, Lazzara L (2019) Reflectance spectra classification for the rapid assessment of water ecological quality in Mediterranean ports. Oceanologia 61(4):445–459

Mehdi MR, Kim M, Seong JC, Arsalan MH (2011) Spatio-temporal patterns of road trafc noise pollution in Karachi, Pakistan. Environ Int 37:97–104. https://doi.org/10.1016/j.envint.2010.08.003

Milczarek W (2019) Application of a small baseline subset time series method with atmospheric correction in monitoring results of mining activity on ground surface and in detecting induced seismic events. Remote Sens 11(9):1008

Minnullina A, Vasiliev V (2018) Determining the supply of material resources for high-rise construction: scenario approach. In: E3S web of conferences 33. EDP Sciences

Monjezi M, Hasanipanah M, Khandelwal M (2013) Evaluation and prediction of blast-induced ground vibration at Shur River Dam, Iran, by artificial neural network. Neural Comput Appl 22(7–8):1637–1643

Monserud RA, Leemans R (1992) Comparing global vegetation maps with the Kappa statistic. Ecol Model 62:275–293

Mossa J, James LA (2013) Impacts of mining on geomorphic systems. In: Treatise on geomorphology, vol 13, pp 74–95. Geomorphology of human disturbances, climate change, and natural hazards. Academic Press, San Diego, CA

Mudenda L (2018) Assessment of water pollution arising from copper mining in Zambia: a case study of Munkulungwe stream in Ndola, Copperbelt province. Doctoral dissertation, University of Cape Town

Mugade UR, Sapkale JB (2015) Influence of aggradation and degradation on river channels: a review. Int J Eng Tech Res 3(6):209–212

Naghibi SA, Ahmadi K, Daneshi A (2017) Application of support vector machine, random forest, and genetic algorithm optimized random forest models in groundwater potential mapping. Water Resour Manage 31 (9):2761–2775

Nayyeri H, Zandi S (2018) Evaluation of the effect of river style framework on water quality: application of geomorphological factors. Environ Earth Sci 77 (9):343

Okafor FO, Egbe EA (2017) Models for predicting compressive strength and water absorption of laterite-quarry dust cement block using mixture experiment. Niger J Technol 36(2):366–372

Omoti K, Kitetu J, Keriko JM (2016) An assessment of the impacts of gypsum mining on water quality in Kajiado County, Kenya. Kabarak J Res Innov 4 (1):91–104

Ozcan O, Musaoglu N, Seker DZ (2012) Environmental impact analysis of quarrying activities established on and near a river bed by using remotely sensed data. Fresenius Environ Bull 21(11):3147–3153

Padmalal D, Maya K, Sreebha S, Sreeja R (2008) Environmental effects of river sand mining: a case from the river catchments of Vembanad lake, Southwest Coast of India. Environ Geol 54(4):879–889

Pal S, Debanshi S (2018) Influences of soil erosion susceptibility toward overloading vulnerability of the gully head bundhs in Mayurakshi River basin of eastern Chottanagpur Plateau. Environ Dev Sustain 20 (4):1739–1775

Pal S, Mandal I (2017) Impacts of stone mining and crushing on stream characters and vegetation health of Dwarka River basin of Jharkhand and West Bengal, Eastern India. J Environ Geogr 10(1–2):11–21

Pal S, Mandal I (2019a) Impacts of stone mining and crushing on environmental health in Dwarka river basin. Geocarto Int 1–29

Pal S, Mandal I (2019b) Impact of aggregate quarrying and crushing on socio-ecological components of Chottanagpur plateau fringe area of India. Environ Earth Sci 78(23):661

Pal S, Mandal I (2021) Noise vulnerability of stone mining and crushing in Dwarka river basin of Eastern India. Environ Dev Sustain 1–22

Pal S, Mahato S, Sarkar S (2016) Impact of fly ash on channel morphology and ambient water quality of Chandrabhaga River of Eastern India. Environ Earth Sci 75:1268

Peña-Ortega M, Del Rio-Salas R, Valencia-Sauceda J, Mendívil-Quijada H, Minjarez-Osorio C, Molina-Freaner F, Moreno-Rodríguez V (2019) Environmental assessment and historic erosion calculation of abandoned mine tailings from a semi-arid zone of northwestern Mexico: insights from geochemistry and unmanned aerial vehicles. Environ Sci Pollut Res 26 (25):26203–26215

Preciso E, Salemi E, Billi P (2012) Land use changes, torrent control works and sediment mining: effects on channel morphology and sediment flux, case study of the Reno River (Northern Italy). Hydrol Process 26 (8):1134–1148

Qi J, Liu X, Yao X, Zhang R, Chen X, Lin X, Liu R (2018) The concentration, source and deposition flux of ammonium and nitrate in atmospheric particles during dust events at a coastal site in northern China. Atmos Chem Phys 18(2):571–586

Quinn R, Avis O, Decker M, Parker A, Cairncross S (2018) An assessment of the microbiological water quality of sand dams in southeastern Kenya. Water 10 (6):708

Ramesh V, Korwar GR, Mandal UK, Prasad JV, Sharma KL, Yezzu SR, Kandula V (2008) Influence of fly ash mixtures on early tree growth and physicochemical properties of soil in semi-arid tropical Alfisols. Agrofor Syst 73(1):13–22

Rasyid AR, Bhandary NP, Yatabe R (2016) Performance of frequency ratio and logistic regression model in creating GIS based landslides susceptibility map at Lompobattang Mountain, Indonesia. Geoenviron Disasters 3(1):19

Sadeghi SH, Gharemahmudli S, Kheirfam H, Darvishan AK, Harchegani MK, Saeidi P, Vafakhah M (2018) Effects of type, level and time of sand and gravel mining on particle size distributions of suspended sediment. Int Soil Water Conserv Res 6(2):184–193

Saha DC, Padhy PK (2011) Effects of stone crushing industry on Shorea robusta and Madhuca indica foliage in Lalpahari forest. Atmos Pollut Res 2(4):463–476

Samah A, Shaffril HAM, Hamzah A, Samah B (2019) Factors affecting small-scale fishermen's adaptation toward the impacts of climate change: reflections from Malaysian fishers. SAGE Open 9(3):2158244019 864204

Sami M, Shiekhdavoodi MJ, Pazhohanniya M, Pazhohanniya F (2014) Environmental comprehensive assessment of agricultural systems at the farm level using fuzzy logic: a case study in cane farms in Iran. Environ Model Softw 58:95–108

Singh R, Rishi MS, Sidhu N (2016) An overview of environmental impacts of riverbed mining in Himalayan terrain of Himachal Pradesh. J Appl Geochem 18(4):473

Sreebha S, Padmalal D (2011) Environmental impact assessment of sand mining from the small catchment rivers in the southwestern coast of India: a case study. Environ Manage 47(1):130–140

Toy TJ, Hadley RF (1987) Geomorphology and reclamation of disturbed lands. United States. https://www.osti.gov/biblio/5769696

Trujillo-González J, Mahecha-Pulido J, Torres-Mora M, Brevik E, Keesstra S, Jiménez-Ballesta R (2017) Impact of potentially contaminated river water on agricultural irrigated soils in an equatorial climate. Agriculture 7(7):52

Turowski JM (2018) Alluvial cover controlling the width, slope and sinuosity of bedrock channels. Earth Surf Dyn 6(1):29-48

USGS (2018) Water Density, The USGS Water Science School, U.S. Department of the Interior. https://www.usgs.gov/special-topic/water-science-school/science/water-density?qt-science_center_objects=0#qt-science_center_objects. Retrived on 15th Sept 2019 at 01:43 AM

Van Duc B, Kennedy O (2018) Adsorbed complex and laboratory geotechnics of Quarry Dust (QD) stabilized lateritic soils. Environ Technol Innov 10:355–363

Wang JM, Yang XG, Zhou HW, Lin X, Jiang R, Lv EQ (2018) Bed morphology around various solid and flexible grade control structures in an unstable gravel-bed river. Water 10(7):822

Wiejaczka Ł, Tamang L, Piróg D, Prokop P (2018) Socioenvironmental issues of river bed material extraction in the Himalayan piedmont (India). Environ Earth Sci 77(20):718

Wilkinson BH, McElroy BJ (2007) The impact of humans on continental erosion and sedimentation. Geol Soc Am Bull 119(1–2):140–156

Xiang J, Chen J, Sofia G, Tian Y, Tarolli P (2018) Open-pit mine geomorphic changes analysis using multi-temporal UAV survey. Environ Earth Sci 77(6):220

Xu J, Zhao H, Yin P, Bu N, Li G (2019) Impact of underground coal mining on regional landscape pattern change based on life cycle: a case study in Peixian, China. Pol J Environ Stud 28(6)

Yanar TA (2003) The enhancement of the cell-based GIS analysis with fuzzy processing capabilities. MSs thesis. The Middle East Technical University

Youssef AM, Pourghasemi HR, Pourtaghi ZS, Al-Katheeri MM (2016) Landslide susceptibility mapping using random forest, boosted regression tree, classification and regression tree, and general linear models and comparison of their performance at Wadi Tayyah Basin, Asir Region, Saudi Arabia. Landslides 13 (5):839–856

Zadeh LA (1965) Fuzzy sets. Inf Control 8(3):338–353